A peer-reviewed version of this preprint was published in PeerJ on 14 December 2016.

View the peer-reviewed version (peerj.com/articles/2766), which is the preferred citable publication unless you specifically need to cite this preprint.

Hu Z, Ma R. 2016. Distribution and characteristic of nitrite-dependent anaerobic methane oxidation bacteria by comparative analysis of wastewater treatment plants and agriculture fields in northern China. PeerJ 4:e2766 https://doi.org/10.7717/peerj.2766

Distribution and characteristic of nitrite-dependent anaerobic methane oxidation bacteria in wastewater treatment plants and agriculture fields of northern China

Zhen Hu Corresp., [1] , **Ru Ma** [1]

[1] School of Environmental Science and Engineering, Shandong University, Jinan, China

Corresponding Author: Zhen Hu
Email address: huzhen885@sdu.edu.cn

Nitrite-dependent anaerobic methane oxidation (n-damo) is a recently discovered biological process, which has been arousing global attention because of its potential in minimizing greenhouse gases emissions. In this study, molecular biological techniques and potential n-damo activity batch experiments were conducted to investigate the presence and diversity of *M. oxyfera* bacteria in paddy field, corn field, and wastewater treatment plant (WWTP) of northern China, as well as lab-scale n-damo enrichment culture. N-damo enrichment culture showed the highest abundance of *M. oxyfera* bacteria and positive correlation was observed between potential n-damo rate and abundance of *M. oxyfera* bacteria. Both paddy field and corn field were believed to be better inoculum than WWTP for the enrichment of *M. oxyfera* bacteria, due to their higher abundance and diversity of *M. oxyfera* bacteria. Comparative analysis revealed that long biomass retention time and optimum environment (low NH_4^+ and high NO_2^- content) were suitable for the growth of *M. oxyfera* bacteria. In addition, the distribution and diversity of *M. oxyfera* bacterial might be related to geographical regions.

Distribution and characteristic of nitrite-dependent anaerobic methane oxidation bacteria by comparative analysis of wastewater treatment plants and agriculture fields in northern China

Zhen Hu[a,*], Ru Ma [a]

[a] School of Environmental Science and Engineering, Shandong University, Jinan, Shandong, China.

Corresponding Author:

Zhen Hu

No. 27 Shanda South Road, Jinan, Shandong 250100,China

E-mail: huzhen885@sdu.edu.cn

Introduction

Methane (CH_4) and nitrous oxide (N_2O) are two of the most important greenhouse gases, accounting for about 20% and 7% of global warming, respectively (Griggs & Noguer 2002; Knittel & Boetius 2009). Cai (2012) reported that anthropogenic activities, rather than natural sources, are the major sources of CH_4 and N_2O emissions. And it is widely accepted that wastewater treatment plants (WWTPs) and agricultural fields are two of the most important anthropogenic GHGs sources (Foley et al. 2011; Liu et al. 2014a). In WWTPs, enormous amount of CH_4 and N_2O would be produced during the biological transformation of carbohydrates and nitrogenous compounds. Our previous on-site investigation of a typical full-scale WWTP of northern China showed that CH_4 and N_2O emission factors of WWTP were 11.3 g CH_4 person^{-1} yr^{-1} and 1.96 g N_2O person^{-1} yr^{-1}, respectively (Wang et al. 2011a; Wang et al. 2011b). Compared with WWTPs, agricultural field is believed to be a more important GHGs sources, mainly because the widely use of fertilizers (IPCC, 2001). It is reported that agriculture field would contribute to 60% of N_2O and 50% of CH_4 emissions on a global scale (Montzka et al. 2011; Syakila & Kroeze 2011).

Anaerobic methane oxidation (AMO) is a recently discovered sink of methane on earth, with a consumption rate of approximately 70–300 Tg CH_4 year^{-1} globally (Cui et al. 2015; Hu et al. 2011). Expect for AMO coupled to sulfate (Barnes & Goldberg 1976; Bian et al. 2001), humic compound (Smemo & Yavitt

2007), iron (Beal et al. 2009; Segarra et al. 2013) and manganese (Egger et al. 2015), the coupling of AOM to nitrite reduction process, named nitrite-dependent anaerobic methane oxidation (n-damo), has also been demonstrated (Raghoebarsing et al. 2006). N-damo process was performed by "*Candidatus* Methylomirabilis oxyfera" (*M. oxyfera*), affiliated with the NC10 phylum (Ettwig et al. 2010). N-damo process established a unique relationship between carbon cycle and nitrogen cycle (Raghoebarsing et al. 2006), and it was believed to be a promising method to minimize greenhouse gases emissions through converting CH_4 and N_2O to CO_2 and N_2, respectively (Raghoebarsing et al. 2006; Shen et al. 2015).

Presently, many studies have been focused on the distribution *of M. oxyfera* bacteria in natural environment, e.g, freshwater lakes (Liu et al. 20 verified 14b), paddy soil (Wang et al. 2012), marine sediments (Chen et al. 2014), wetlands (Hu et al. 2014b), and etc. However, to date, information about distribution of *M. oxyfera* bacteria in northern China is still lacking. In addition, various inoculums have been reported to be able to successfully enrich *M. oxyfera* bacteria, including freshwater sediment (Raghoebarsing et al. 2006), sewage treatment sludge (Luesken et al. 2011a), ditch sediments (Ettwig et al. 2009) and paddy soil (Shen et al. 2014a; Wang et al. 2012). He et al. (2014) found that inoculum sources had significant effect on enrichment of *M. oxyfera* bacteria, and claimed that paddy soil was the optimal inoculum. However, intensive study on inoculum sources from the perspective of microorganism is absence.

In this study, the diversity and abundance of *M. oxyfera* bacteria in four different sites of northern China,

i.e., paddy field, corn field, n-damo enrichment culture and WWTP, were investigated through molecular biology analyses. Comparative analysis of environmental features and *M. oxyfera* bacteria activity was conducted to reveal the characteristics of *M. oxyfera* bacteria, and optimal enrichment conditions were also proposed.

Materials and methods

Site description and sample collection

Non-flooded paddy field with rice reaping once per year (PF) and corn field with maize-wheat rotation for over 50 years (CF), both of which are typical agricultural type of northern China, were selected as agricultural field sample sites. PF cores and CF cores were collected from three locations (5m distance) at the 50cm-60cm depth in each sampling site, according to the previously described methods (Hu et al. 2014b). Sludge from anaerobic tank of local WWTP (Everbright Water, Jinan China) (WS), and lab-scale Upflow Anaerobic Sludge Bed reactor (UASB) aiming at enrichment of *M.oxyfera* bacteria (EC), were selected as WWTP samples. The sample collection was conducted in October, 2015, and the environmental characteristics of each sample site were listed in Table 1.

All collected samples were placed in hermetic containers and immediately transported to the laboratory

within 4h. Subsequently, the collected samples were equally divided into three parts. The first part was placed in the incubator to measure the potential n-damo rates, the second parts was stored in refrigerator at 4℃ for analysis of physicochemical parameters, and the last part was stored in refrigerator at -20℃ for further microbiological analysis.

Table 1. *Environmental characteristics of the sample sites*

Physicochemical parameters analysis

Soil samples were extracted with 1M KCl and the concentrations of ammonium, nitrite and nitrate were measured as described by Ryan et al. (2007). Soil pH was measured at soil/water ratio of 1:2.5 using a pH analyzer (HQ30d 53LEDTM, HACH, USA) (Wang et al. 2012). Temperature and salinity of soil was measured in *situ* using HI98331 soil electrical conductivity meter (HANNA, Shanghai).

Concentrations of ammonium, nitrite and nitrate in water samples were analyzed according to the standard method (APHA 2005). Water temperature, pH and salinity were measured in *situ* using pH and salinity analyzer (DDBJ-350, Leici, Shanghai). And CH_4 concentration was analyzed using gas chromatograph equipped with flame ionization detector (FID–GC) (7890B, GC system, Agilent Technologies).

Potential n-damo activity batch experiment

All the samples were washed three times with anaerobic water to remove the residual NO_x^- (NO_2^- and NO_3^-)

and organic compounds, and were then transferred to 1L Ar-flushed glass bottles. The soil slurries were pre-incubated under anoxic conditions for at least 48 h to recover the microbial activity, and then flushed with Ar gas again before the measurement of potential n-damo activity. Two treatment groups were conducted subsequently: (a) CH_4 (blank group, CH_4 at 99%), (b) CH_4+NO_2^-(experimental group). The initial CH_4 concentrations in both blank and experimental groups were 1.02 ± 0.06 mmol L^{-1} and the initial concentrations of NO_2^- in the experimental groups were 0.35 ± 0.01 mmol NO_2^- L^{-1}. The variation of CH_4 and NO_2^- concentrations were determined at intervals of 6 hours. The potential methane oxidation rates and the ratio of CH_4/NO_2^- were evaluated by linear regression of the concentrations of decreased CH_4 and NO_2^- in the experimental groups.

Fluorescence in situ hybridization (FISH)

Approximately 0.3g of collected samples were washed in phosphate-buffered saline (PBS; 10 mM Na_2HPO_4/NaH_2PO_4 pH 7.5 and 130 mM NaCl) and fixed with 4% (w/v) paraformaldehyde in PBS for 3h under 4℃. After incubation, the sediment (fixed biomass) was washed with PBS and then stored in mixture (1ml) of ethanol and PBS (1×) at −20 °C until analysis.

Bacterial probe S-*-DBACT-1027-a-A-18 (5'-TCTCCACGCTCCCTTGCG-3') (Cy3, red), specific for bacteria affiliated with the NC10 phylum were used in this study (Raghoebarsing et al. 2006); and a mixture of

EUB I-III (FITC, green) was used for the detection of total bacteria (Daims et al. 1999). Fixed biomass (10 μl) was spotted on microscopic slides circles and then dehydrated subsequently with 50%, 80%, and 98% of ethanol for 3min each. The probes were hybridized for 2 h at 46 °C in hybridization buffer (5M NaCl, 1M Tris/HCl pH 8.0, 10% sodium dodecyl sulfate) and 40% formamide. Hybridized samples were washed with hybridization leachate at 48℃ and then added with the fluorescence decay resistance agent. Fluorescence microscope (Olympus BX53, Japan) was used to observe the prepared slides and the picture was disposed with software Image-Pro Plus 6.0.

DNA extraction and PCR amplification

Total DNA was extracted using Power Soil DNA Isolation kit (Mo Bio Laboratories, Carlsbad, CA) according to the manufacturer's protocols. And DNA concentration was measured at 260nm with Nano-drop spectrophotometer (Nano-Drop Technologies, USA).

To understand the biodiversity of *M. oxyfera* bacteria, 16S rRNA gene and *pmoA* gene of *M. oxyfera* bacteria were amplified using nested PCR protocols, as previously described (Hu et al. 2014b; Luesken et al. 2011b). Nested PCR was that the first PCR products were then used as the DNA templates in the following nested PCR. For 16S rRNA gene amplification, specific forward primer 202F (Ettwig et al. 2009) and general bacterial reverse primer 1545R (Juretschko et al. 1998) were used for the first round, NC10 specific primers

qP1F and qP2R (Ettwig et al. 2009) were performed for the second round. For *pmoA* gene amplification, forward primer A189_b and reverse primer cmo682 (Luesken et al. 2011b) were used in the first PCR, and the primer cmo182 and cmo568 were used in the second PCR (Luesken et al. 2011b). The detailed information of nested PCR is shown in Table S1.

Quantitative Real-Time PCR (qPCR)

The quantitative PCR of *M. oxyfera* bacteria 16S rRNA gene were performed on LightCycler480 with Sequence Detection Software v1.4 (Applied Biosystems, USA). The abundance of 16S rRNA gene was determined using the primers qp1R-qp1F (Ettwig et al. 2009) with 10 μL of Power SYBR Green PCR Master Mix (Applied BioSystems), 1 μL of template DNA (5–20 ng μL^{-1}), 0.4 μL of each primer and 8.2 μL of ddH_2O. Detailed information is exhibited in Table S1. Negative-control reactions in which the DNA template was replaced by nuclease-free water were also performed. The whole process was performed under sterile conditions on ice and away from light. Triplicate qPCR analyses were performed for each sample. The standard curve was constructed from purified plasmid DNA with the concentrations ranging from 1.0×10^1 to 1.0×10^7 copies μL^{-1}, and it showed correlation between the DNA template concentration and the crossing point with coefficients of determination (R^2>0.97). The qPCR amplification efficiency of the standard curve and reactions were both greater than 85%.

Sequencing and phylogenetic analyses

Nucleotide sequences of *M.oxyfera* bacteria were recovered by 454 high-throughput sequencing (16S rRNA gene) and Illumina MiSeq sequencing (*pmoA* gene), both of which were accomplished by Shanghai Personalbio-pharm Technology Co., Ltd (Shanghai, China). Sequences were clustered into operational taxonomic unites (OTUs) by UCLUST (Edgar et al. 2011). Chao1 richness estimator, ACE estimator, Simpson diversity and Good's coverage were calculated in Mothur analysis (http://www.mothur.org). Sequences analyses were operated by BLAST searching to obtain related sequences (>90% identity) from NCBI (http://www.ncbi.nlm.nih.gov/GenBank/) and sequence identity was performed in Clustal W version 2.1. Phylogenetic trees were established with MEGA 4.0 software (Tamura et al. 2007) using neighbor-joining method with *p* distance correction and a 1,000-replicate bootstrap value (Hu et al. 2014a).

Nucleotide sequence accession numbers

Sequences obtained from these samples were divided into 16S rRNA and *pmoA* of *M. oxyfera*, and were submitted to GenBank under accession numbers KX153190-KX153201 and KX153202-KX153210, respectively.

Ethical Statement This article does not contain any studies with human participants or animals performed

by any of the authors.

Results

Physicochemical Characteristics of the Sample Sites

Significant differences in physicochemical characteristics among different environmental samples were observed in the present study. The peak NH_4^+-N content (815.88 mg N kg^{-1} dry sediment) was detected in WS, which was over 80-folds higher than that in the other three sample sites. And highest NO_2^--N content (14120 mg N kg^{-1} dry sediment) was observed in EC, while NO_2^--N content in the other three sample site varied form 0.37-127.19 mg N kg^{-1} dry sediment. Mainly because of its high NO_2^- content, the highest NO_x^--N content was also observed in EC, which was beyond 17-folds higher than that of the other three sample sites. In addition, compared with published research conducted in paddy field, where NO_X^--N content was around 1.4 -3.3 mg N kg^{-1} dry sediment (Shen et al. 2014a; Zhou et al. 2014 ; Ding et al. 2015), higher NO_X^--N content (27.72 and 46.81 mg N kg^{-1} dry sediment) in the agriculture field (PF and CF) of northern China were observed in this study, mainly caused by difference in farming methods.

Abundance of M.oxyfera bacteria

FISH analysis was used to investigate the spatial distribution and relative quantification of *M. oxyfera* bacteria compared to total bacteria. As shown in Fig. 1, *M. oxyfera* bacteria (represented by red color) were observed in all four sample sites, and the proportion of *M. oxyfera* bacteria to total bacteria followed the order of EC>PF>CF>WS. Notably, compared with total bacteria, *M.oxyfera* bacteria in the enrichment culture took up over 50%, indicating the predominance of *M.oxyfera* bacteria.

To further accurately quantify the abundance of *M. oxyfera* bacteria, qPCR analysis was conducted and significant difference was also observed in different sampling sites. The abundance of *M. oxyfera* bacteria were $7.28\pm0.8\times10^{7}$,$1.55\pm0.3\times10^{7}$, $1.07\pm0.3\times10^{10}$, $2.61\pm0.1\times10^{6}$ copies per gram of dry sediment in PF, CF, EC and WS, respectively (Fig.2). This order was in consistence with results of FISH analysis.

Fig. 1 *FISH image of the collected samples. The M. oxyfera bacteria was hybridized with probe S-*-DBACT-1027-a-A-18(Cy3, red) and total bacteria was hybridized with probes EUB I-III (FITC, green). a&e, PF; b&f, CF; c&g, EC, d&h, WS. The scale bar indicates 100 μm.*

Fig. 2 *The abundance of M. oxyfera bacteria in different sample sites.*

Potential Rates of n-damo Activity

In order to estimate the activity of *M. oxyfera* bacteria, two groups of experiments were operated using the collected samples, and the results are shown in Fig. 3. In experimental groups amended with CH_4 and NO_2^-,

dramatic decline in CH_4 concentration were observed compared with the blank groups, indicating that CH_4 oxidation was propelled by NO_2^- reduction under anoxic conditions. The detected anaerobic methane oxidizing rates were 3.90±0.05, 2.58±0.08, 22.31±0.02 and 1.61±0.01 μmol CH_4 g^{-1} d^{-1} in PF, CF, EC and WS, respectively. The stoichiometric ratio for methane to nitrite, calculated through the curve fitting method, were 3:5.7 for PF, 3:4.6 for CF, 3:6.9 for EC, and 3:3.2 for WS. The value of n-damo enrichment culture was the closest to the theoretical stoichiometric ratio, which was 3:8 (Ettwig et al. 2010).

Fig. 3 *The consumption rates of methane and nitrite in the paddy field (a), corn field (b), n-damo enrichment culture (c), WWTP (d).*

Sequencing analysis of M. oxyfera bacteria 16S rRNA gene

In order to estimate the distribution and composition of *M. oxyfera* bacteria, 454 high-throughput sequencing analysis of 16S rRNA gene was conducted. Raw reads obtained from four libraries ranged from 11017 to 14814 and the good coverage values varied from 86.48% to 94.70% (Table S2), indicating that these sequences were enough to analyze the microbial communities. The number of OTUs, Chao1 estimator, ACE estimator, Shannon index and Simpson index based on 97% of the similar level were calculated (Table S2) to estimate the community diversity.

The composition of bacteria community in four samples was described at the phylum level (Fig. S1). Some

sequences that could not be divided into any known group were classified into others. The first 7 phyla obtained in four sample sites were *NC10*, *Acido*bacteria, *Armatimonadetes*, *Firmicutes*, *Proteo*bacteria, *Nitrospirae*, *Verrucomicrobia*. *NC10, Acido*bacteria and *Armatimonadetes* were recognized as dominant phyla since them accounting for 93.25% to 99.14% of total bacteria in all samples. For the better understanding of the diversity of *M. oxyfera* bacteria, phylogenetic tree based on selecting all the sequences related to *Candidatus* 'Methylomirabilis oxyfera' (similarities to *M. oxyfera* >90 %) was constructed and is shown in Fig. 4. Sequences of *M. oxyfera* bacteria 16S rRNA gene were grouped into two groups according to Ettwig et al.(2009) Sequences of group A, which were obtained from PF, CF, EC and WS, showed identity of 94.84-99.31%, 94.20-99.17%, 94.47-99.31%, and 94.16-99.31% to the 16S rRNA gene of *M. oxyfera* bacteria, respectively. Sequences of group B, acquired from the EC showed identity of 89.15% to the 16S rRNA gene of *M. oxyfera* bacteria.

Fig. 4 *Phylogenetic tree showing the phylogenetic affiliations of M. oxyfera bacteria 16S rRNA sequences in different sample sites by neighbor-joining method. Bootstrap values were 1,000 replicates and the scale bar represents 2% of the sequence divergence.*

Sequencing analysis of M. oxyfera bacteria pmoA gene

The Illumina MiSeq sequencing analysis was used to detect the *pmo*A genes of *M. oxyfera* bacteria on a

functional level. Raw reads obtained from four libraries ranged from 63,186 to 96,276 and good's coverage varied from 93.91 to 98.13%, indicating that the obtained sequences were able to confirm the bacteria community structure on a functional level. The number of OTUs, Chao1 estimator, ACE estimator, Shannon index and Simpson index based on 97% of the similar level were shown in Table S2.

The sequences, which were similar to the *pmo*A gene of *M. oxyfera*, were obtained to construct phylogenetic tree, as shown in Fig. 5. Sequences recovered from PF, CF, EC and WS showed 89.76-91.4%, 90.3-92.7%, 89.8-91.4%, 90.3-91.4% of similarity to the *pmo*A gene of *M. oxyfera* bacteria, respectively.

Fig. 5 *Neighbor-joining phylogenetic tree showing the phylogenetic affiliations of M. oxyfera bacteria pmoA gene sequences in different sample sites. Bootstrap values were 1,000 replicates and the scale bar represents 5% of the sequence divergence.*

Discussion

In the present study, PF, CF, EC and WS in northern China, as previously overlooked sites, were selected to investigate the presence and characteristics of n-damo process. Results showed that EC had the highest potential n-damo rate, as well as the highest abundance of *M. oxyfera* bacteria. Correlation analysis showed that the potential n-damo rates and the abundance of *M. oxyfera* bacteria followed the same descending order, i.e., EC>PF>CF>WS, indicating positive correlation between the two indexes. Moreover, the measured

potential n-damo rate (22.31±0.02 μ mol CH_4 $g^{-1}d^{-1}$) in EC of the present study was higher than that reported in other n-damo enrichment culture (0.8±0.1 μ mol CH_4 $h^{-1}g^{-1}$VSS) (He et al. 2014). This was attributed to the relative higher abundance of *M. oxyfera* bacteria in the present study. The abundance of *M. oxyfera* bacteria in the present study was over 20 times higher than that reported by He et al. (2014), which verifed the positive correlation between the potential n-damo rates and the abundance of M. oxyfera bacteria on the other hand.

WWTP showed lower abundance of *M. oxyfera* bacteria than the other three sample sites, mainly because of its short biomass retention time (13 days), while biomass retention time of other three sample sites was years or even decades of years (Kampman et al. 2014; Weiland BP. 2006). With the doubling time of 1–2 weeks (Ettwig et al. 2009), the growth rate of *M. oxyfera* bacteria is very low, indicating that *M. oxyfera* bacteria might be washed out in WWTP and resulted in lower abundance of M. oxyfera bacteria. Another possible reason was that high NH_4^+ content in WWTP, which was unfavorable for the growth of *M. oxyfera* bacteria. Winkler et al. (2015) found that the anammox bacteria had advantage over *M. oxyfera* bacteria for nitrite in the presence of excess ammonium. What is more interesting, although WS was used as initial inoculum for EC in this study, the abundance of *M. oxyfera* bacteria in EC was over 4×10^3 times higher than that in WS. This was mainly attributed to a combination of low NH_4^+ content and high NO_2^- content during the enrichment period in EC. It was reported that the nitrite affinity constant of was 0.6 g NO_2^-- Nm^{-3},

237 indicating that high NO_2^- content was more beneficial for the growth of *M .oxyfera* bacteria (Winkler et al.
238 2015).

239 The diversity of *M. oxyfera* bacteria was determined by 16S rRNA gene sequencing analysis. Group A of
240 *M. oxyfera* bacteria, which were the dominant bacteria responsible for conducting the n-damo process (Ettwig
241 et al. 2009; Hu et al. 2009; Luesken et al. 2011a), were obtained in all four sample sites, whereas the group B
242 members were primarily recovered from EC. Sequencing analysis found that diversity of *M. oxyfera* bacteria
243 in PF and CF was higher than that in WS. There is no doubt that PF and CF were believed to be better
244 inoculum to enrich *M. oxyfera* bacteria due to their higher abundance and diversity of *M. oxyfera* bacteria.
245 Notably, with WS used as initial inoculum, increase of 3 OTUs was observed in n-damo EC after cultivation.
246 Besides the optimum enrichment culture in EC, i.e., low NH_4^+ and high NO_2^- contents, which was favorable
247 for the growth of *M. oxyfera* bacteria, the increase in diversity might also be attributed to the longer biomass
248 retention time of EC.

249 The diversity of *M.oxyfera* bacteria *pmo*A gene observed in agriculture fields (PF and CF) were 6 and 7
250 OTUs, respectively, which were higher than most of the previously examined freshwater habitats, including
251 wetland (Hu et al. 2014b; Shen et al. 2015), paddy soil (Shen et al. 2014a) and lake (Deutzmann & Schink
252 2011). And, phylogenetic analysis showed that all the OTUs of *M.oxyfera* bacteria *pmoA* genes in natural
253 environment samples (i.e., PF, CF and WS) of the present study have close genetic relationship with Yellow

River basin sediment. Results of 16S rRNA gene sequencing analysis also showed that over half of the OTUs of *M.oxyfera* bacteria 16S rRNA gene obtained in natural environment samples were genetically belongs to the Yellow River basin sediment. This indicated that the diversity of *M. oxyfera* bacteria might be related to geographical regions. Different geographical region has specific environmental conditions, including salinity (Chen et al. 2014), temperature (Hu et al. 2009), pH (He et al. 2015), and etc., all of which would affect the diversity of *M.oxyfera* bacteria. However, further research and more direct evidence are needed to get this conclusion.

In conclusion, the present study further expanded our knowledge on distribution and characteristic of *M. oxyfera* bacteria in northern China. Comparative analysis showed that long biomass retention time and optimum environment (i.e., low NH_4^+ and high NO_2^- contents) would benefit the growth of *M. oxyfera* bacteria. The diversity of *M. oxyfera* bacteria might also be related to geographical regions. In addition, positive correlation between abundance of *M. oxyfera* bacteria and potential n-damo activity rate were observed.

References

APHA. 2005. Standard methods for the examination of water and wastewater. *American Public Health Association (APHA): Washington, DC, USA*.

Barnes RO, and Goldberg ED. 1976. Methane production and consumption in anoxic marine sediments. Geology 4. 10.1130/0091-7613(1976)4<297:mpacia>2.0.co;2

Bian L, Hinrichs K-U, Xie T, Brassell SC, Iversen N, Fossing H, Jørgensen BB, and Hayes JM. 2001. Algal and archaeal polyisoprenoids in a recent marine sediment: Molecular isotopic evidence for anaerobic oxidation of methane. Geochemistry, Geophysics, Geosystems 2:n/a-n/a. 10.1029/2000gc000112

Cai Z. 2012. Greenhouse gas budget for terrestrial ecosystems in China. *Science China Earth Sciences* 55:173-182. 10.1007/s11430-011-4309-8

Chen J, Jiang X-W, and Gu J-D. 2014. Existence of Novel Phylotypes of Nitrite-Dependent Anaerobic Methane-Oxidizing Bacteria in Surface and Subsurface Sediments of the South China Sea. *Geomicrobiology Journal* 32:1-10. 10.1080/01490451.2014.917742

Cui M, Ma A, Qi H, Zhuang X, and Zhuang G. 2015. Anaerobic oxidation of methane: an “active” microbial process. *MicrobiologyOpen* 4:1-11. 10.1002/mbo3.232

Daims H, Brühl A, Amann R, Schleifer K-H, and Wagner M. 1999. The Domain-specific Probe EUB338 is Insufficient for the Detection of all Bacteria: Development and Evaluation of a more Comprehensive Probe Set. *Systematic and Applied Microbiology* 22:434-444. 10.1016/s0723-2020(99)80053-8

Deutzmann JS and Schink B. 2011. Anaerobic oxidation of methane in sediments of Lake Constance, an oligotrophic freshwater lake. Appl Environ Microbiol. p 4429-4436.

Ding J, Fu L, Ding ZW, Lu YZ, Cheng SH and Zeng RJ. 2015. "Environmental evaluation of coexistence of denitrifying anaerobic methane-oxidizing archaea and bacteria in a paddy field." Appl Microbiol Biotechnol 100(1): 439-446.

Edgar RC, Haas BJ, Clemente JC, Quince C, and Knight R. 2011. UCHIME improves sensitivity and speed of chimera detection. *Bioinformatics* 27:2194-2200.

Egger M, Rasigraf O, Sapart CJ, Jilbert T, Jetten MSM, Röckmann T, van der Veen C, Bândă N, Kartal B, Ettwig KF, and Slomp CP. 2015. Iron-Mediated Anaerobic Oxidation of Methane in Brackish Coastal

293 Sediments. Environmental Science & Technology 49:277-283. 10.1021/es503663z

294 Emily J. Beal CHH, Victoria J. Orphan. 2009. Manganese- and Iron-Dependent Marine Methane Oxidation.

295 Ettwig KF, Butler MK, Le Paslier D, Pelletier E, Mangenot S, Kuypers MM, Schreiber F, Dutilh BE, Zedelius

296 J, de Beer D, Gloerich J, Wessels HJ, van Alen T, Luesken F, Wu ML, van de Pas-Schoonen KT, Op

297 den Camp HJ, Janssen-Megens EM, Francoijs KJ, Stunnenberg H, Weissenbach J, Jetten MS, and

298 Strous M. 2010. Nitrite-driven anaerobic methane oxidation by oxygenic bacteria. *Nature* 464:543-

299 548. 10.1038/nature08883

300 Ettwig KF, van Alen T, van de Pas-Schoonen KT, Jetten MSM, and Strous M. 2009. Enrichment and

301 Molecular Detection of Denitrifying Methanotrophic Bacteria of the NC10 Phylum. *Applied and*

302 *Environmental Microbiology* 75:3656-3662. 10.1128/aem.00067-09

303 Foley JA, Ramankutty N, Brauman KA, Cassidy ES, Gerber JS, Johnston M, Mueller ND, O'Connell C, Ray

304 DK, West PC, Balzer C, Bennett EM, Carpenter SR, Hill J, Monfreda C, Polasky S, Rockstrom J,

305 Sheehan J, Siebert S, Tilman D, and Zaks DP. 2011. Solutions for a cultivated planet. *Nature* 478:337-

306 342. 10.1038/nature10452

307 Griggs DJ, and Noguer M. 2002. Climate change 2001: the scientific basis. Contribution of working group I to

308 the third assessment report of the intergovernmental panel on climate change. *Weather* 57:267-269.

309 He Z, Cai C, Shen L, Lou L, Zheng P, Xu X, and Hu B. 2014. Effect of inoculum sources on the enrichment of

310 nitrite-dependent anaerobic methane-oxidizing bacteria. *Appl Microbiol Biotechnol* 99:939-946.

311 10.1007/s00253-014-6033-8

312 Hu B, He Z, Geng S, Cai C, Lou L, Zheng P, and Xu X. 2014a. Cultivation of nitrite-dependent anaerobic

313 methane-oxidizing bacteria: impact of reactor configuration. *Appl Microbiol Biotechnol* 98:7983-7991.

314 10.1007/s00253-014-5835-z

315 Hu BL, Shen LD, Lian X, Zhu Q, Liu S, Huang Q, He ZF, Geng S, Cheng DQ, Lou LP, Xu XY, Zheng P, and
316 He YF. 2014b. Evidence for nitrite-dependent anaerobic methane oxidation as a previously
317 overlooked microbial methane sink in wetlands. *Proc Natl Acad Sci U S A* 111:4495-4500.
318 10.1073/pnas.1318393111
319 Hu S, Zeng RJ, Burow LC, Lant P, Keller J, and Yuan Z. 2009. Enrichment of denitrifying anaerobic methane
320 oxidizing microorganisms. *Environmental Microbiology Reports* 1:377-384.
321 Hu S, Zeng RJ, Keller J, Lant PA, and Yuan Z. 2011. Effect of nitrate and nitrite on the selection of
322 microorganisms in the denitrifying anaerobic methane oxidation process. *Environ Microbiol Rep*
323 3:315-319. 10.1111/j.1758-2229.2010.00227.x
324 Intergovernmental Panel on Climate Change (IPCC), *Third Assessment Report. Working Group I,* Cambridge
325 Univ. Press, New York, 2001.
326 Juretschko S, Timmermann G, Schmid M, Schleifer K-H, Pommerening-Röser A, Koops H-P, and Wagner M.
327 1998. Combined molecular and conventional analyses of nitrifying bacterium diversity in activated
328 sludge: Nitrosococcus mobilis and Nitrospira-like bacteria as dominant populations. *Applied and*
329 *environmental microbiology* 64:3042-3051.
330 Kampman C, Temmink H, Hendrickx TLG, Zeeman G, and Buisman CJN. 2014. Enrichment of denitrifying
331 methanotrophic bacteria from municipal wastewater sludge in a membrane bioreactor at 20°C. *Journal*
332 *of Hazardous Materials* 274:428-435. 10.1016/j.jhazmat.2014.04.031
333 Knittel K, and Boetius A. 2009. Anaerobic Oxidation of Methane: Progress with an Unknown Process.
334 *Annual Review of Microbiology*, 311-334.
335 Liu Y, Cheng X, Lun X, and Sun D. 2014a. CH4 emission and conversion from A2O and SBR processes in
336 full-scale wastewater treatment plants. *Journal of Environmental Sciences* 26:224-230.

http://dx.doi.org/10.1016/S1001-0742(13)60401-5

Liu Y, Zhang J, Zhao L, Li Y, Yang Y, and Xie S. 2014b. Aerobic and nitrite-dependent methane-oxidizing microorganisms in sediments of freshwater lakes on the Yunnan Plateau. *Appl Microbiol Biotechnol* 99:2371-2381. 10.1007/s00253-014-6141-5

Luesken FA, van Alen TA, van der Biezen E, Frijters C, Toonen G, Kampman C, Hendrickx TLG, Zeeman G, Temmink H, Strous M, Op den Camp HJM, and Jetten MSM. 2011a. Diversity and enrichment of nitrite-dependent anaerobic methane oxidizing bacteria from wastewater sludge. *Appl Microbiol Biotechnol* 92:845-854. 10.1007/s00253-011-3361-9

Luesken FA, Zhu B, van Alen TA, Butler MK, Diaz MR, Song B, Op den Camp HJM, Jetten MSM, and Ettwig KF. 2011b. pmoA Primers for Detection of Anaerobic Methanotrophs. *Applied and Environmental Microbiology* 77:3877-3880. 10.1128/aem.02960-10

Montzka SA, Dlugokencky EJ, and Butler JH. 2011. Non-CO2 greenhouse gases and climate change. *Nature* 476:43-50. 10.1038/nature10322

Raghoebarsing AA, Pol A, van de Pas-Schoonen KT, Smolders AJ, Ettwig KF, Rijpstra WI, Schouten S, Damste JS, Op den Camp HJ, Jetten MS, and Strous M. 2006. A microbial consortium couples anaerobic methane oxidation to denitrification. *Nature* 440:918-921. 10.1038/nature04617

Ryan J, Estefan G, and Rashid A. 2007. *Soil and plant analysis laboratory manual*: ICARDA.

Segarra KEA, Comerford C, Slaughter J, and Joye SB. 2013. Impact of electron acceptor availability on the anaerobic oxidation of methane in coastal freshwater and brackish wetland sediments. Geochimica et Cosmochimica Acta 115:15-30. 10.1016/j.gca.2013.03.029

Shen L-d, Liu S, He Z-f, Lian X, Huang Q, He Y-f, Lou L-p, Xu X-y, Zheng P, and Hu B-l. 2015. Depth-specific distribution and importance of nitrite-dependent anaerobic ammonium and methane-oxidising

359 bacteria in an urban wetland. *Soil Biology and Biochemistry* 83:43-51.
360 http://dx.doi.org/10.1016/j.soilbio.2015.01.010
361 Shen L-d, Liu S, Huang Q, Lian X, He Z-f, Geng S, Jin R-c, He Y-f, Lou L-p, and Xu X-y. 2014a. Evidence
362 for the cooccurrence of nitrite-dependent anaerobic ammonium and methane oxidation processes in a
363 flooded paddy field. *Applied and environmental microbiology* 80:7611-7619.
364 Shen L-d, Qun Z, Shuai L, Ping D, Jiang-ning Z, Dong-qing C, Xiang-yang X, Ping Z, and Bao-lan H. 2014b.
365 Molecular evidence for nitrite-dependent anaerobic methane-oxidising bacteria in the Jiaojiang
366 Estuary of the East Sea (China). *Appl Microbiol Biotechnol* 98:5029-5038. 10.1007/s00253-014-5556-
367 3
368 Smemo KA, and Yavitt JB. 2007. Evidence for Anaerobic CH4 Oxidation in Freshwater Peatlands.
369 Geomicrobiology Journal 24:583-597. 10.1080/01490450701672083
370 Syakila A, and Kroeze C. 2011. The global nitrous oxide budget revisited. *Greenhouse Gas Measurement and*
371 *Management* 1:17-26. 10.3763/ghgmm.2010.0007
372 Tamura K, Dudley J, Nei M, and Kumar S. 2007. MEGA4: molecular evolutionary genetics analysis (MEGA)
373 software version 4.0. *Molecular biology and evolution* 24:1596-1599.
374 Wang J, Zhang J, Wang J, Qi P, Ren Y, and Hu Z. 2011a. Nitrous oxide emissions from a typical northern
375 Chinese municipal wastewater treatment plant. *Desalination and Water Treatment* 32:145-152.
376 10.5004/dwt.2011.2691
377 Wang J, Zhang J, Xie H, Qi P, Ren Y, and Hu Z. 2011b. Methane emissions from a full-scale A/A/O
378 wastewater treatment plant. *Bioresource Technology* 102:5479-5485. 10.1016/j.biortech.2010.10.090
379 Wang Y, Zhu G, Harhangi HR, Zhu B, Jetten MSM, Yin C, and Op den Camp HJM. 2012. Co-occurrence and
380 distribution of nitrite-dependent anaerobic ammonium and methane-oxidizing bacteria in a paddy soil.

FEMS Microbiology Letters 336:79-88. 10.1111/j.1574-6968.2012.02654.x

Weiland BP. 2006. Biomass Digestion in Agriculture: A Successful Pathway for the Energy Production and Waste Treatment in Germany. Engineering in Life Sciences 6:302-309. 10.1002/elsc.200620128

Winkler MKH, Ettwig KF, Vannecke TPW, Stultiens K, Bogdan A, Kartal B, and Volcke EIP. 2015. Modelling simultaneous anaerobic methane and ammonium removal in a granular sludge reactor. *Water Research* 73:323-331. 10.1016/j.watres.2015.01.039

Zhou LL, Wang Y, Long XE, Guo JH, Zhu GB. 2014. "High abundance and diversity of nitrite-dependent anaerobic methane-oxidizing bacteria in a paddy field profile." FEMS Microbiology Letters 360(1): 33-41.

Table 1(on next page)

Environmental characteristics

Environmental characteristics of the sample sites.

Distribution and characteristic of nitrite-dependent anaerobic methane oxidation bacteria in wastewater treatment plants and agriculture fields of northern China

Ru Ma . Zhen Hu*

Shandong Provincial Key Laboratory of Water Pollution Control and Resource Reuse, School of Environmental Science and Engineering, Shandong University, No. 27 Shanda South Road, Jinan 250100, Shandong, People's Republic of China. E-mail: huzhen885@sdu.edu.cn

Table 1. Environmental characteristics of the sample sites.

Sample sites	Geographic coordinates	Temperature (℃)	pH	Ammonium (mg N/kg dry sed)	Nitrite (mg N/kg dry sed)	Nitrate (mg N/kg dry sed)	Salinity (‰)
PF	N36° 41', E116° 54'	17	7.3	10.34	0.75	26.97	1.8
CF	N37° 44', E115° 40'	15	7.0	2.627	0.37	46.44	1.1
EC	N36° 40', E117° 03'	32	7.0	0.125	14117.65	941.18	1.2
WS	N36° 42', E117° 02'	22	7.6	815.88	127.19	735.29	2.1

Figure 1(on next page)

FISH image of the collected samples.

Fig. 1- FISH image of the collected samples. The *M. oxyfera* bacteria was hybridized with probe S-*-DBACT-1027-a-A-18(Cy3, red) and total bacteria was hybridized with probes EUB I-III (FITC, green). a&e, PF; b&f, CF; c&g, EC, d&h, WS. The scale bar indicates 100 µm.

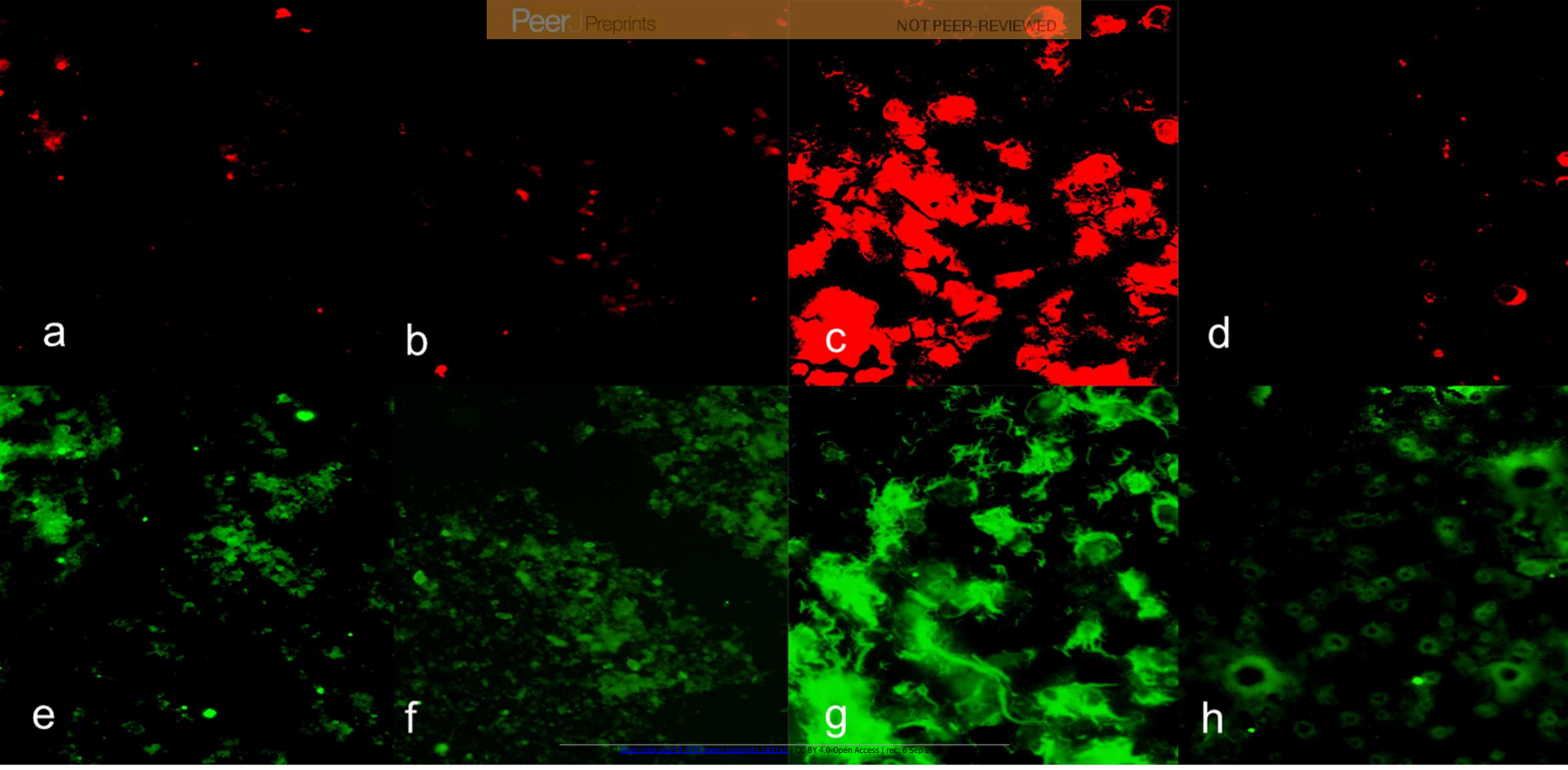

Figure 2(on next page)

Q-PCR Image of *M. oxyfera* bacteria

Fig. 2- The abundance of *M. oxyfera* bacteria 16S rRNA gene copy numbers of collected samples.

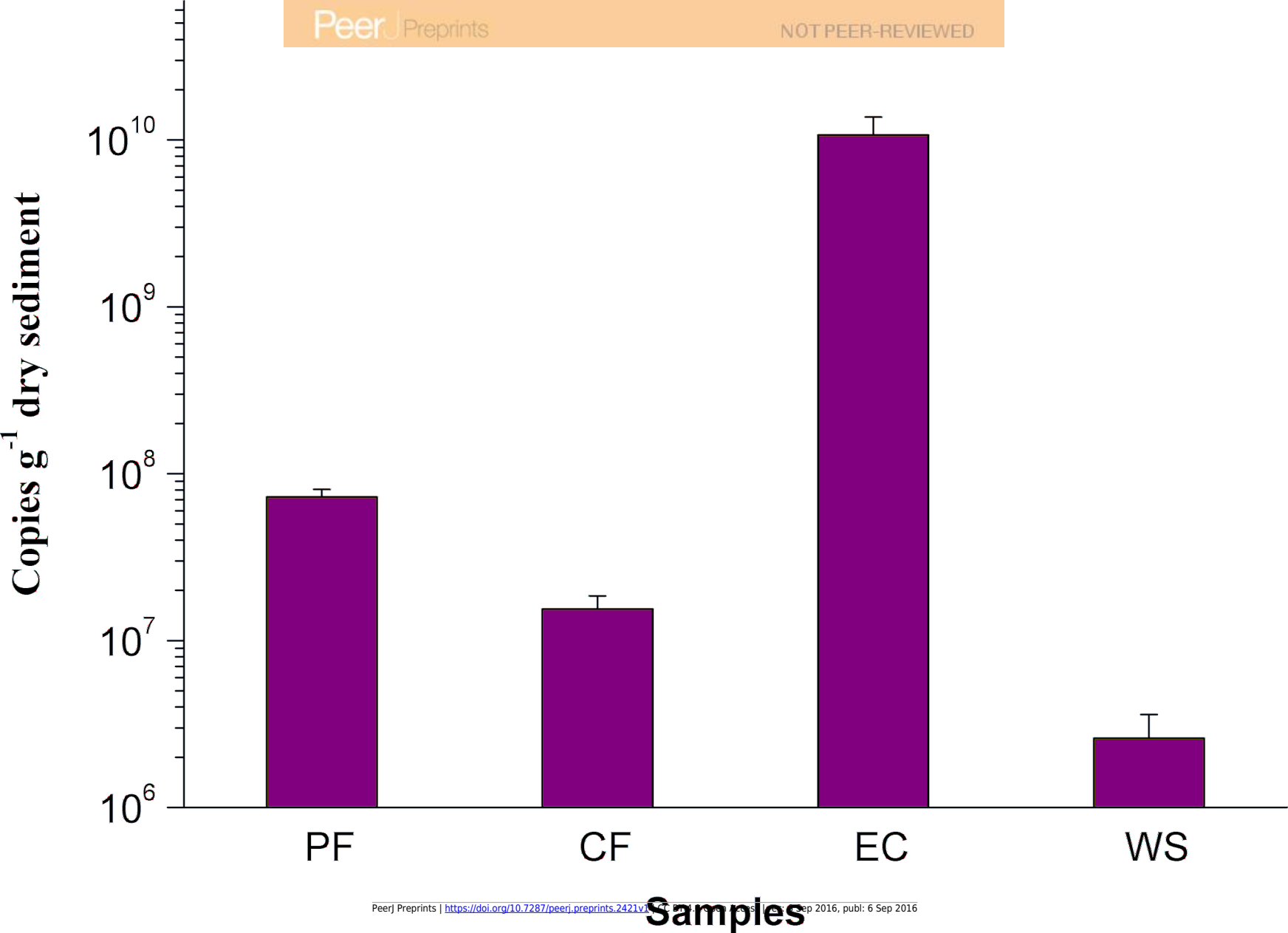

PeerJ Preprints | https://doi.org/10.7287/peerj.preprints.2421v1 | CC-BY 4.0 Open Access | rec: 6 Sep 2016, publ: 6 Sep 2016

Figure 3(on next page)

Image of batch test

Fig. 3 The consumption rates of methane and nitrite in the paddy field (a), corn field (b), n-damo enrichment culture (c), WWTP (d).

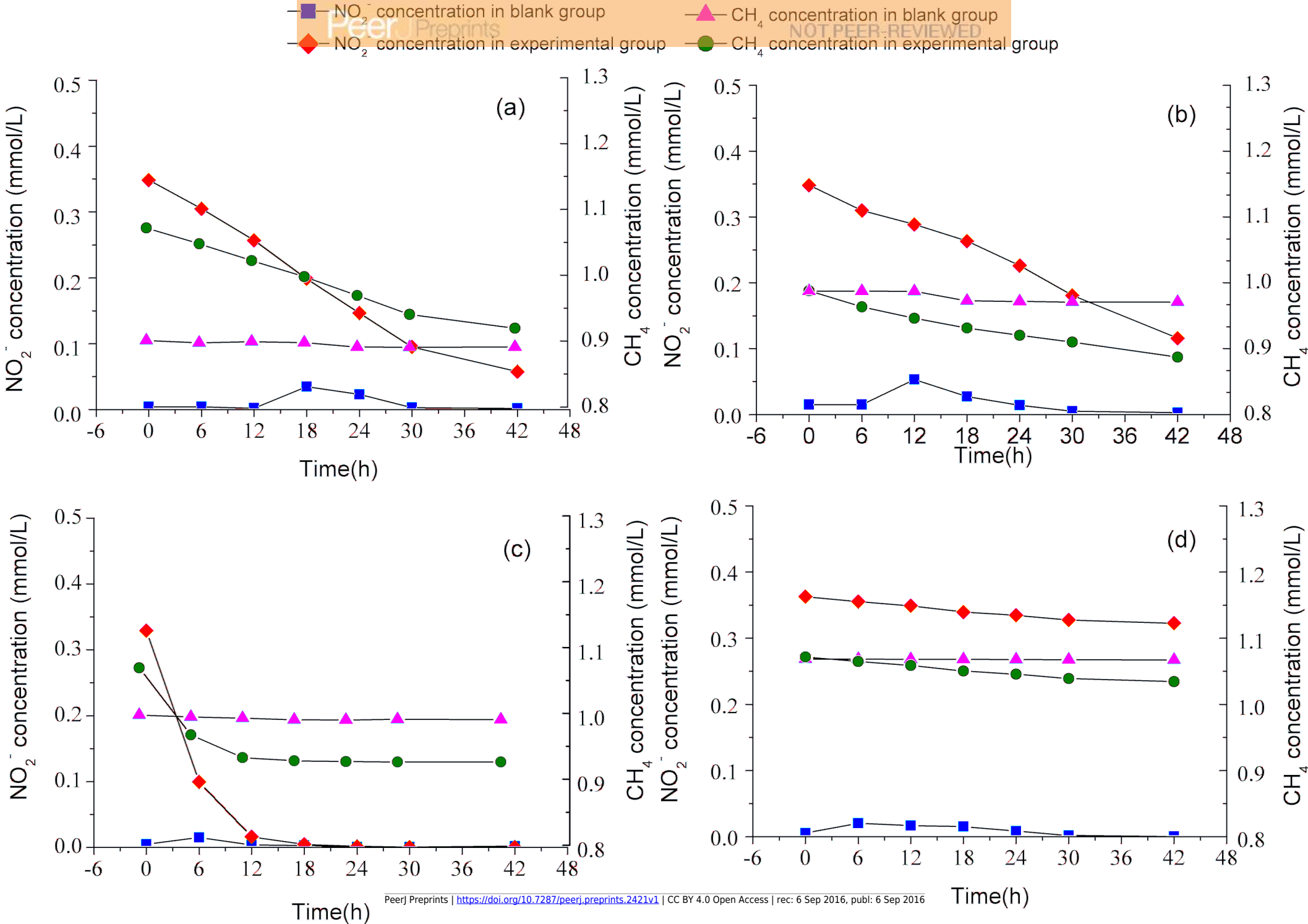

PeerJ Preprints | https://doi.org/10.7287/peerj.preprints.2421v1 | CC BY 4.0 Open Access | rec: 6 Sep 2016, publ: 6 Sep 2016

Figure 4(on next page)

Phylogenetic tree of *M. oxyfera* bacteria 16S rRNA sequences

Fig. 4 - Phylogenetic tree showing the phylogenetic affiliations of *M. oxyfera* bacteria 16S rRNA sequences in four samples by neighbor-joining method. Bootstrap values were 1,000 replicates and the scale bar represents 2% of the sequence divergence.

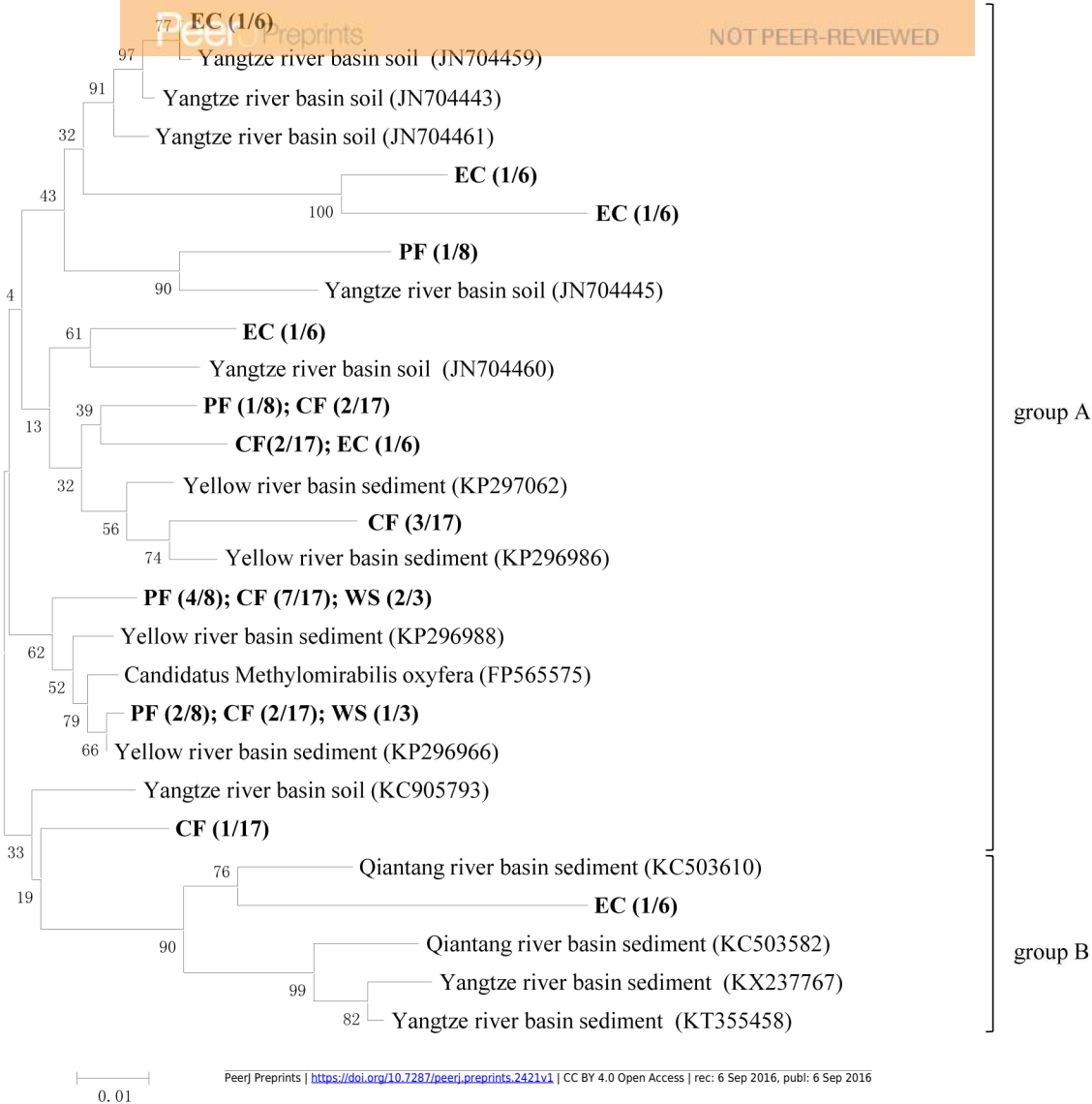

PeerJ Preprints | https://doi.org/10.7287/peerj.preprints.2421v1 | CC BY 4.0 Open Access | rec: 6 Sep 2016, publ: 6 Sep 2016

Figure 5(on next page)

Phylogenetic tree of *M. oxyfera* bacteria *pmoA* gene

Fig. 5 - Neighbor-joining phylogenetic tree showing the phylogenetic affiliations of *M. oxyfera* bacteria *pmoA* gene sequences in four samples. Bootstrap values were 1,000 replicates and the scale bar represents 5% of the sequence divergence.

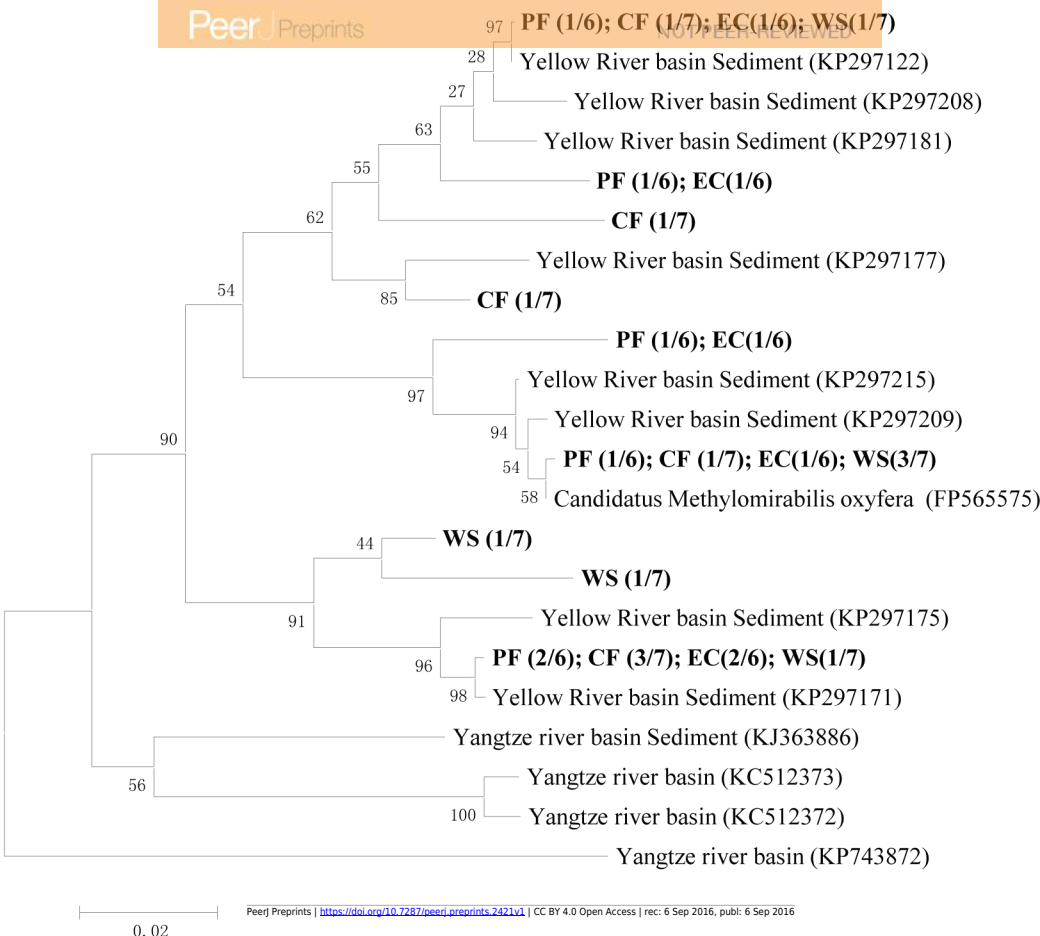

PeerJ Preprints | https://doi.org/10.7287/peerj.preprints.2421v1 | CC BY 4.0 Open Access | rec: 6 Sep 2016, publ: 6 Sep 2016